Resources, Conservation & Recycling 184 (2022) 106413

Contents lists available at ScienceDirect

Resources, Conservation & Recycling

journal homepage: www.elsevier.com/locate/resconrec

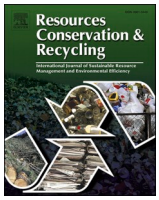

Full length article

Valorization of urban and marine PET waste by optimized chemical recycling

Eider Mendiburu-Valor [a], Gurutz Mondragon [a], Nekane González [b], Galder Kortaberria [a], Loli Martin [c], Arantxa Eceiza [a,*], Cristina Peña-Rodriguez [a,*]

[a] 'Materials+Tecnologies' Research group, Chemistry and Environmental Engineering Department, Faculty of Engineering, University of the Basque Country (UPV/EHU), Plaza Europa 1, Donostia, Gipuzkoa 20018, Spain
[b] Antex, Josep Hereu i Aulet 8, Anglés 17160, Spain
[c] Macrobehaviour-Mesostructure-Nanotechnology SGIker Service, Faculty of Engineering, University of Basque Country (UPV/EHU), Plaza Europa, 1, Donostia-San Sebastián 20018, Spain

ARTICLE INFO

Keywords:
PET waste
Degradation
Glycolysis
Pressure reactor
BHET
Recycling

ABSTRACT

The degradation of two poly(ethylene terephtalate) (PET) samples from urban and marine wastes (PET-u and PET-m, respectively) has been studied by comparing their properties with those of virgin PET (PET-v) and post-condensed PET for bottle fabrication (PET-ssp). FTIR spectroscopy, DSC analysis, WCA and MFI results have confirmed that all PET residues were degraded. Therefore, the chemical recycling has been evaluated in order to valorize PET-m and PET-u wastes, analyzing the effect of degradation on the process. Glycolysis of degraded and non-degraded PET samples has been carried out in a pressure reactor at 220°C for 30 min. For all the cases almost pure BHET monomer has been obtained: 96.5 and 96.7 % for PET-m and PET-u respectively, values 2 and 13 % higher than those obtained for PET-ssp and PET-v. Obtained results indicate that the initial degradation of PET wastes increases the BHET monomer content in the glycolyzed sample.

1. Introduction

Plastics are one of the most abundant type of materials used worldwide, and their production is continuously growing. As an example, within an estimated global production of plastics of around 368 million tons per year, Europe produced around 57.9 million tons of plastic during 2019 (PlasticsEurope, 2020). This high plastic production leads to the generation of a large amount of waste. As plastics show usually high physical and chemical stability, their natural degradation can take thousands of years (Barnes et al., 2009). A big portion of plastic wastes end up at the sea, with the consequent danger for the marine environment. It is estimated that around 12.2 million tons per year end up in the sea (Plastics Recyclers Europe, 2020). The most common plastic wastes found at seas and oceans are polypropylene (PP) and PET (Iñiguez et al., 2018b).

PET is a semicrystalline thermoplastic polyester employed in the manufacture of fibers to produce fabrics and sheets, in the manufacture of food packaging, and also for multi-layer materials in not-packaging applications. Among the most commonly polymers employed for food and beverage packaging, PET is the most appropriate one, due to its physic-chemical stability (Chapa-Martínez et al., 2016) and good barrier properties. PET present good mechanical and thermal properties and, therefore, it is also used for the production of plastic reinforcements (del Mar Castro López et al., 2014). Besides due to the great flexibility, as well as low cost, this polyester is one of the responsible for the plastic consumption increase in recent years (Wei et al., 2017). In 2000 the global demand for this material was of around 6.4 million tons, with a growth rate of 6.9 %, while 10 years later, in 2010, this demand was almost the double, reaching around 12.6 million tons. According to the latest data, in 2020 the global demand has been estimated to be of around 23.4 million tons, with a growth rate of 6.4 % (Chemie, 2020). As a result, the volume of wastes continuously increases, becoming more necessary the development of optimized recycling processes for obtaining raw materials for the production of new products or for the energy recovery.

According to a study carried out by Plastic Recyclers Europe, Unesda, Petcore Europe and Natural Mineral Waters Europe, 4.6 million tons of PET residues were generated in Europe in 2020 (Plastics Recyclers Europe et al., 2022), from which only the 49 % (1.9 million tons) were collected and sorted for recycling (Plastics Recyclers Europe et al.,

* Corresponding authors.
E-mail addresses: arantxa.eceiza@ehu.eus (A. Eceiza), cristina.pr@ehu.eus (C. Peña-Rodriguez).

https://doi.org/10.1016/j.resconrec.2022.106413
Received 29 December 2021; Received in revised form 12 May 2022; Accepted 16 May 2022
Available online 24 May 2022

2022). About the rest 51 %, most of the waste ends up in incineration or land-fill plants, and an important part ends up in the sea. However, the management and recycling of marine waste is more complicated than that of urban solid waste. On one hand, the collection of this waste is complicated and on the other hand, the quality of the material to be recycled is poor, PET becoming a serious problem at seas and oceans. The marine environment degrades materials, changing their properties, constituting a reason for which marine wastes cannot be recycled as urban wastes. The degradation is defined as the partial or complete breakdown of a polymer chain (Iñiguez et al., 2018). The factors that affect the degradation of plastics found in marine environment are the solar radiation, the saltiness of the sea, the atmospheric oxygen, changes in the temperature of the seas and oceans and the friction with waves and other elements as rocks (Iñiguez et al., 2018a; Peña-Rodriguez et al., 2021). Five types of degradation processes can occur in marine environment: hydrolytic, thermo-oxidative, mechanical, biological, and photo-degradation (Iñiguez et al., 2018a).

On the other hand, the glycolysis has been reported as the oldest method for chemical recycling of polymeric wastes (Shojaei et al., 2020). It consists on a solvolytic degradation of PET that reacts with glycols such as EG, DEG or PG, among others, breaking the ester bonds of the polymer chain and replacing them by hydroxyl groups, obtaining different oligomers and finally the bis(2-hydroxyethyl) terephthalate (BHET) monomer (Raheem et al., 2019; Shojaei et al., 2020).

In this work, the degradation of PET beverage bottle wastes, both from marine and urban origin has been analyzed by several physic-chemical techniques, comparing their properties with those of virgin and post-condensed PET, which are the raw material employed for PET bottles fabrication, in order to design an appropriate recycling procedure for these wastes. In this way, the depolymerization of PET samples from different sources has also been carried out in this work, obtaining BHET monomer using a previously optimized short-time glycolysis process (Mendiburu-Valor et al., 2021).

2. Materials and Methods

2.1. Materials, sample preparation and glycolysis process

In this work, four different PET samples have been used. Virgin PET pellets (PET-v) supplied by Plastiverd (Barcelona, Spain), is a transparent and amorphous PET with a viscosity of 0.58 ± 0.04 dl/g from the supplier. Post-condensed PET pellets (PET-ssp) supplied by Indorama (Cádiz, Spain), is a commercial post-condensed virgin PET, an opaque crystalline sample with a viscosity of 0.78 ± 0.05 dl/g from the supplier. As for bottle production PET should present viscosity values between 0.78 and 0.80-dl/g, virgin PET is post-condensed. Urban post-consumer PET waste (PET-u) was provided by Eko-Rec company (Andoain, Spain), obtained from beverage bottles recovered from municipal wastes and milled into flakes. For comparative purpose, commercial PET bottles have been used (PET-bottle) supplied by Nestlé, Aquarel. PET-v and PET-ssp pellets and PET-u flakes were used as received. Marine post-consumer PET waste (PET-m) was directly collected from the coast of the Basque Country, in the flysch zone between Deba and Zumaia (Gipuzkoa, Spain). Collected bottles are shown in Fig. 1, which were washed with tap water, dried for 3 h at 60°C in a vacuum oven and milled into flakes in a grinder for obtaining 2 cm size pellets. It is important to point out that both urban flakes and marine bottles showed huge variety of colors that affects to the final appearance of the glycolysis product. Since humidity can interfere in the characterization or could also provoke hydrolytic degradation during processing resulting in a reduction of the molecular weight (Abbasi et al., 2007a), all samples have been conditioned for 1 h at 50°C in a vacuum oven before any characterization or treatment. Fig. 2 shows the different PET materials studied in this work.

In addition, PET-v, PET-ssp, PET-u and PET-m samples have been compressed using a hydraulic press Santec 30 at 58 bar and 270°C for 10 min in order to analyze the behavior when submit at elevated temperature.

Fig. 1. PET bottles recovered from the sea.

For the glycolysis process, ethylene glycol (EG) from Sigma-Aldrich (EEUU) was used as reactive and chemically pure zinc acetate from PROBUS, C. Busquets (Badalona, Spain) as catalyst. For characterization purposes, standard BHET from Sigma-Aldrich (San Luis, Missouri, USA) and tetrahydrofuran (THF) provided by Macron Fine Chemicals™ (Avantor, Gliwice, Poland) were also used.

Glycolysis reactions have been carried out under a pressure of 3 bar in a 0.3 L Parr 50 mini reactor equipped with a thermometer, a manometer and a refrigeration system. Mechanical stirring was maintained constant at 1000–1200 rpm. A PET/EG weight ratio of 1:3 has been employed (40 g PET, 120 g EG), with 1% mass of zinc acetate as catalyst, in a working volume of approximately 160 ml. As BHET has been obtained at very short times (10 min) according to previous work of our group (Mendiburu-Valor et al., 2021), reactions of 30 min have been carried out in the present work. After placing the reactants into the reactor, it was heated up to 220°C and, once the temperature was reached, reaction time was quantified. The previous warm-up time was variable between 30 and 45 min. After the reaction, excess hot water has been added to the glycolysis product constituted by BHET monomer, low molecular oligomers, and EG as well, and have been left for 24 h at room temperature. After that, the glycolyzed product (G), constituted by BHET monomer (O1), dimer (O2) and oligomers (O3), has been purified from EG by vacuum filtration using glass microfiber filters and washed with plenty of water. Finally, the solid fraction has been dried under vacuum at 50°C for 24 h. Insoluble fractions and yields (η) have been calculated by the procedure reported in our previous work (Mendiburu-Valor et al., 2021). Briefly, THF was added after the glycolysis reaction and soluble components, such as BHET monomer, low molecular weight oligomers and EG, were separated from insoluble fractions by filtration, which were dried and weighted for their evaluation. The reactions were performed in duplicate and the mean value of the yield and standard deviation were calculated from results obtained in triplicate for each of the reactions.

2.2. Characterization techniques

The characteristic functional groups and chemical interactions in PET samples and their respective glycolyzed products have been analyzed by Fourier transform infrared spectroscopy (FTIR). Spectra have been recorded by a Nicolet Nexus spectrometer (Thermo Fisher Scientific, Waltham, Massachusetts, USA) provided with a MKII Golden Gate accessory (Specac) with a diamond crystal at a nominal incidence angle of 45° and ZnSe lens. Spectra have been recorded in attenuated total reflection (ATR) mode between 4000 and 650 cm^{-1}, performing 64 scans with a resolution of 8 cm^{-1}.

Thermal properties of the PET-v and PET-ssp pellets and PET-u and PET-m flakes have been determined by differential scanning calorimetry (DSC). The analysis has been performed in a Mettler Toledo DSC3+ equipment (Columbus, Ohio, USA) provided with a robotic arm and an

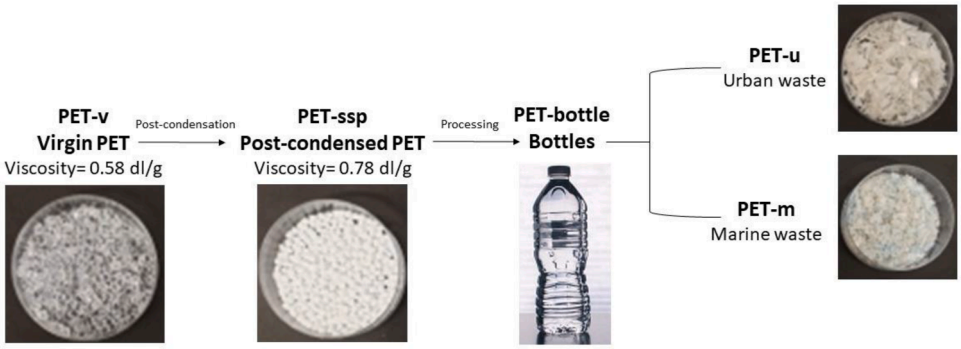

Fig. 2. Digital images of different PET materials analyzed.

electric intracooler as refrigerator unit. Between 5 and 10 mg of sample have been encapsulated in aluminum pans. For the analysis, 3 scans have been carried out under nitrogen atmosphere: a first heating ramp from 25°C up to 300°C, followed by a cooling stage from 300 to 25°C and a second heating ramp up to 300°C, with heating and cooling rates of 10°C/min. From the heating thermograms, glass transition (T_g), crystallization (T_c) and melting temperatures (T_m) have been determined. The T_g has been ascribed to the inflexion point of the heat capacity. The exothermic peak minimum and endothermic peak maximum have been taken as T_c and T_m, respectively. The area of each peak has been considered as the crystallization and melting enthalpy, ΔH_c and ΔH_m, respectively. The degree of crystallinity (Xc) has been calculated by the following equation (Ahani et al., 2016):

$$X_c = \left[\frac{\Delta H_m - \Delta H_c}{\Delta H_0}\right] \cdot 100 \quad (1)$$

The term ΔH_0 is a reference value corresponding to the heat of melting of a 100% crystalline PET (135.8 J/g) (Starkweather et al., 1983). Taking into account the sample variability among PET-u and PET-m, three samples have been analyzed for each of them, estimating the mean value and the standard deviation.

The surface hydrophilicity of PET samples has been measured by static water contact angle (WCA) using the SEO Phoenix Series P-300 equipment (Kromtek Sdn Bhd, Selangor, Malaysia) at room temperature. In this technique, a deionized water drop is deposited at the surface of the sample to measure the contact angle value formed by the water drop, which depends on the chemical interactions between water and the surface. For hydrophilic materials the contact angle is low, increasing with the hydrophobicity. With this purpose, 2 μL of water have been deposited onto the material surface using a 0.4 mm diameter syringe. The contact angle has been measured ten seconds after drop deposition. WCA values of five water drops deposited over the surface prepared by compression molding have been averaged for each sample. Different areas of the compressed plates have been measured.

The melt flow index (MFI) has been measured by using the HAAKE Meltflow^{LT} analyser (Thermo Fisher Scientific, Waltham, Massachusetts, USA). In this technique, the sample is placed in the barrel previously heated at 280°C. According to DIN ISO 1133 standard, 7 g of sample has been placed in the analyser, measuring the time taken by the sample for falling between the established scales, and weighting the mass that has flown in that time. The MFI value has been determined by averaging the values obtained from three tests. As it is reported, there is a relationship between intrinsic viscosity (I.V.) and MFI values (Sanches et al., 2005). Therefore, in order to determinate the I.V. values of PET samples, a calibration straight has been created from MFI and I.V. values, as shown in Eq. (2):

$$[\text{I.V.}] = 1.7956 \cdot MFI^{-0.245} \quad (2)$$

Moreover, weight and number average molecular mass values, M_w and M_n, have been calculated from I.V. values, from the following equations [18]:

$$[\text{I.V.}] = 3.72 \cdot 10^{-4} \cdot M_n^{0.73} \quad (3)$$

$$[\text{I.V.}] = 4.68 \cdot 10^{-4} \cdot M_w^{0.68} \quad (4)$$

Regarding glycolyzed fractions obtained from PET depolymerization, their weight average molecular weight (Mw) and number average molecular weight (Mn) values have been determined by gel permeation chromatography (GPC), using a Thermo Fisher Scientific chromatograph (Waltham, Massachusetts, USA), equipped with an isocratic Dionex UltiMate 3000 pump and a RefractoMax 521 refractive index detector. The separation has been carried out at 30°C within four Phenogel GPC columns from Phenomenex with 5 μm particle size and porosities of 105, 103, 100, and 50 Å, located in an UltiMate 3000 thermostated column compartment. THF was used as mobile phase at a flow rate of 1 mL/min. Samples have been prepared by solving obtained glycolyzed fraction in THF at 1 wt% and filtering using nylon filters with a pore size of 2 μm. Mw and Mn have been reported as weight average based on monodisperse polystyrene standards.

3. Results and discussion

3.1. Materials characterization and degradation analysis

The chemical structure of samples has been analyzed through FTIR, very sensitive to structural changes (Dubelley et al., 2017). Structural changes in PET samples due to environmental degradation and changes in crystallinity or chain conformation have been widely studied in several works (Dubelley et al., 2017; Holland and Hay, 2002; Sammon et al., 2000).

The main bands of PET samples can be seen at the spectra of Fig. 3. The band around the wavenumber of 1712 cm^{-1}, attributed to the C=O stretching vibration, and those around 1240 and 1090 cm^{-1}, corresponding to the asymmetric and symmetric C-O stretching vibrations, respectively, have confirmed the presence of the ester group. Moreover, the band around 1500 cm^{-1}, attributed to the C=C stretching vibration in aromatic rings and those at 870 and 720 cm^{-1}, both attributed to the out-of plane C-H bending in benzene ring, have confirmed the presence of the *para*-substituted aromatic structure of PET (Dubelley et al., 2017; Holland and Hay, 2002). Regarding to PET-v and PET-ssp raw materials, the observed differences could come from their different molecular weight and crystallinity. It is well known that PET should present a minimal viscosity, melt resistance, and proper mechanical properties for being injection processed for bottle production. For this reason, PET-v is post condensed into PET-ssp, in order to increase the molecular weight and achieve the rheological properties required for injection, resulting into crystallinity differences between them (Gantillon et al., 2004). FTIR spectra of amorphous and semicrystalline PET show differences at the CH_2 wagging region, in which bands around 1370 and 1340 cm^{-1}, associated with *gauche* (amorphous) and *trans* (crystalline)

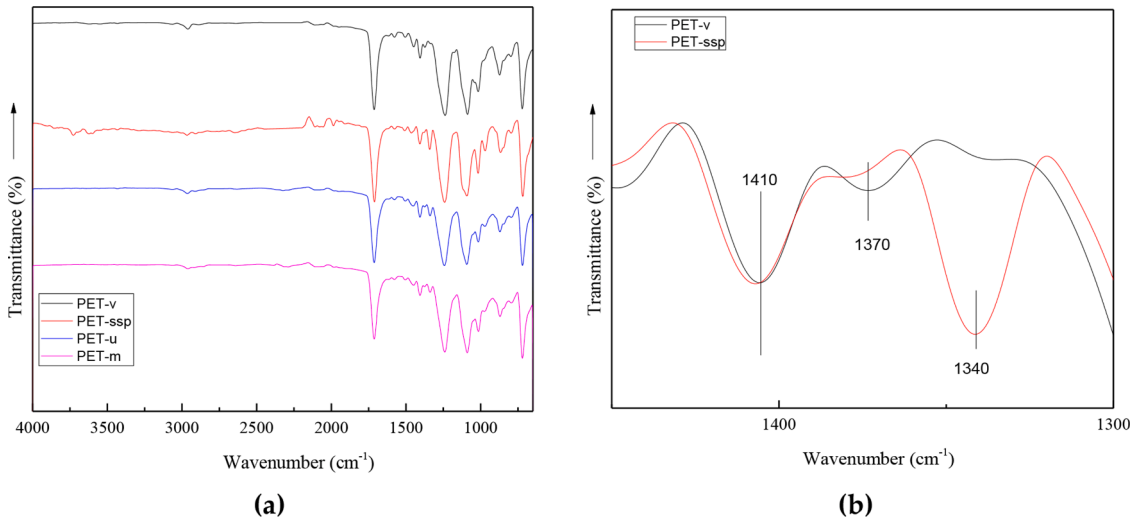

Fig. 3. FTIR spectra of: a) PET-v, PET-ssp, PET-u and PET-m samples and b) PET-v and PET-ssp at the 1450-1300 cm^{-1} interval.

conformations, respectively, can be seen (Dieval et al., 2012). Fig. 3b shows the FTIR spectra of PET-v and PET-ssp at the 1450-1300 cm^{-1} interval, normalized with respect to the in-plane C-H bending band of the benzene ring at 1410 cm^{-1}, since this band has been reported as insensitive to conformational changes (Bertoldo et al., 2010; Zhou et al., 2019). As can be observed in the PET-v spectrum, the band related with the amorphous structure prevails, whereas for PET-ssp the most intense band is related to the crystalline structure.

Comparing the spectra of PET-m and PET-u wastes with that of PET-ssp (used for beverage bottle fabrication), changes related with hydrolytic degradation could be expected, since hydrolysis is the main process occurring at low temperatures, below the glass transition (Pirzadeh et al., 2007). Hydrolysis is a breakdown of water-activated ester bonds with the formation of carboxylic and hydroxyl end groups (Holland and Hay, 2002; Sammon et al., 2000), which causes the cleavage of polymer chains, decreasing the molecular weight. Furthermore, under marine environmental conditions, in addition to hydrolytic degradation, UV-induced photo-oxidation is also a relevant degradation pathway (Gewert et al., 2015). In fact, the ester groups in terephthalate moiety as well as CH_2 groups are strongly involved in the photo-degradation of PET (Fotopoulou and Karapanagioti, 2019). Photo-degradation leads to the cleavage of the ester bond forming as a result carboxylic acid end groups (Gewert et al., 2015; Venkatachalam et al., 2012). As it has been reported several times in the literature the hydrolysis and photo-oxidation degradations have similar degradation pathways (Fotopoulou and Karapanagioti, 2019; Gewert et al., 2015). Therefore, both photo-oxidative and hydrolysis can cause changes in the FTIR spectrum at the vibration stretching intervals of hydroxyl and carbonyl groups, together with that of C-O-C of ester group and CH_2 (Fig. 4).

At the interval corresponding to the stretching vibration of hydroxyl group (Fig. 4a), in addition to the band around 3450 cm^{-1} related with O-H stretching vibration of ethylene glycol end groups (Holland and Hay, 2002), PET-u and PET-m showed a broad band around 3260 cm^{-1} associated to hydrogen-bonded O-H groups from carboxylic and alcoholic end groups (Sammon et al., 2000). As it has been reported in the literature this band broadens with degradation suggesting the presence of carboxylic acids (Edge et al., 1996). Among PET wastes, the intensity of this band is higher for PET-m sample, suggesting that this sample could be more degraded due to the higher hydrolytic and photo-degradation aggressiveness of marine environment. At this interval, some other bands related with aromatic and aliphatic C-H stretching vibrations around 3060 cm^{-1} and 2970 cm^{-1} wavenumbers, respectively, can be observed. At the interval corresponding to the stretching vibration of carbonyl groups (Fig. 4b), the intensity of the carbonyl band of the ester group at 1712 cm^{-1} decreased in PET-u and PET-m samples compared to that of PET-ssp. Furthermore, this band widens towards lower wavenumbers, which is usually attributed to the stretching vibration of the carbonyl group of the carboxylic acid (Dubelley et al., 2017). At the third interval (Fig. 4c), the intensity of the ester group C-O-C band at 1240 cm^{-1} decreased in PET-u and PET-ssp. PET-ssp sample shows a shoulder at 1120 cm^{-1}, which has been attributed to *trans* (crystalline) ethylene glycol (Cole et al., 2002; Dubelley et al., 2017). This shoulder is missing for PET-u and PET-m, agreeing with their lower crystallinity when compared to PET-ssp. Moreover, the band attributed to the in plane bending of C-H in benzene ring at 1015 cm^{-1}, which has been found to increase with crystallinity as consequence of annealing or drawing (Bertoldo et al., 2010; Cole et al., 2002), decreased in PET-u and PET-m samples.

As it was previously discussed, the CH_2 wagging region is useful to analyse PET crystallinity. As can be seen in FTIR spectra of Fig. 4d, corresponding to that region, the ratio between intensities of the trans (crystalline) band around 1340 cm^{-1} and the band at 1410 cm^{-1} taken as reference, I1340/I1410, decreased for both PET-u and PET-m, in agreement with previous results. Despite the bands related with hydroxyl, carboxylic acid and ester carbonyls suggested that higher chain excision occurred in PET-m, its crystallinity seems to be lower than that of PET-u. However, it should be taken into account that after the fabrication of beverage bottles by injection molding from PET-ssp, the fast cooling process applied results into lower crystallinity. Fig. 4d also shows the FTIR spectra of a piece taken from a bottle of PET (PET-bottle) for comparative purposes. As can be observed the I1340/I1410 ratio of PET-bottle is considerably lower than that of PET-ssp. Therefore, the lower I1340/I1410 ratio observed in PET-u and PET-m residues coming from bottles comparing to PET-ssp could be mainly related to the processing.

So, it can be deduced that the more degraded samples such as PET-u and PET-m present lower crystallinity than PET-ssp, but quite similar to PET-bottle, as it has been shown by FTIR analysis.

Thermal properties of post-consumer and marine PET wastes may change when compared to those of PET-ssp and PET-v, due to hydrolytic degradation (Abbasi et al., 2007b; Masmoudi et al., 2018a; Pegoretti and Penati, 2004; Qin et al., 2018). Fig. 5 shows the most representative DSC thermograms of different PET samples, corresponding to the first heating, cooling and second heating scans. The values of thermal properties obtained from them are summarized in Table 1.

During the first heating scan, a T_g at 70°C, an exothermic crystallization peak (T_c) at 126°C and an endothermic melting peak (T_m) at 252°C have been detected for PET-v sample, whereas for PET-ssp one no

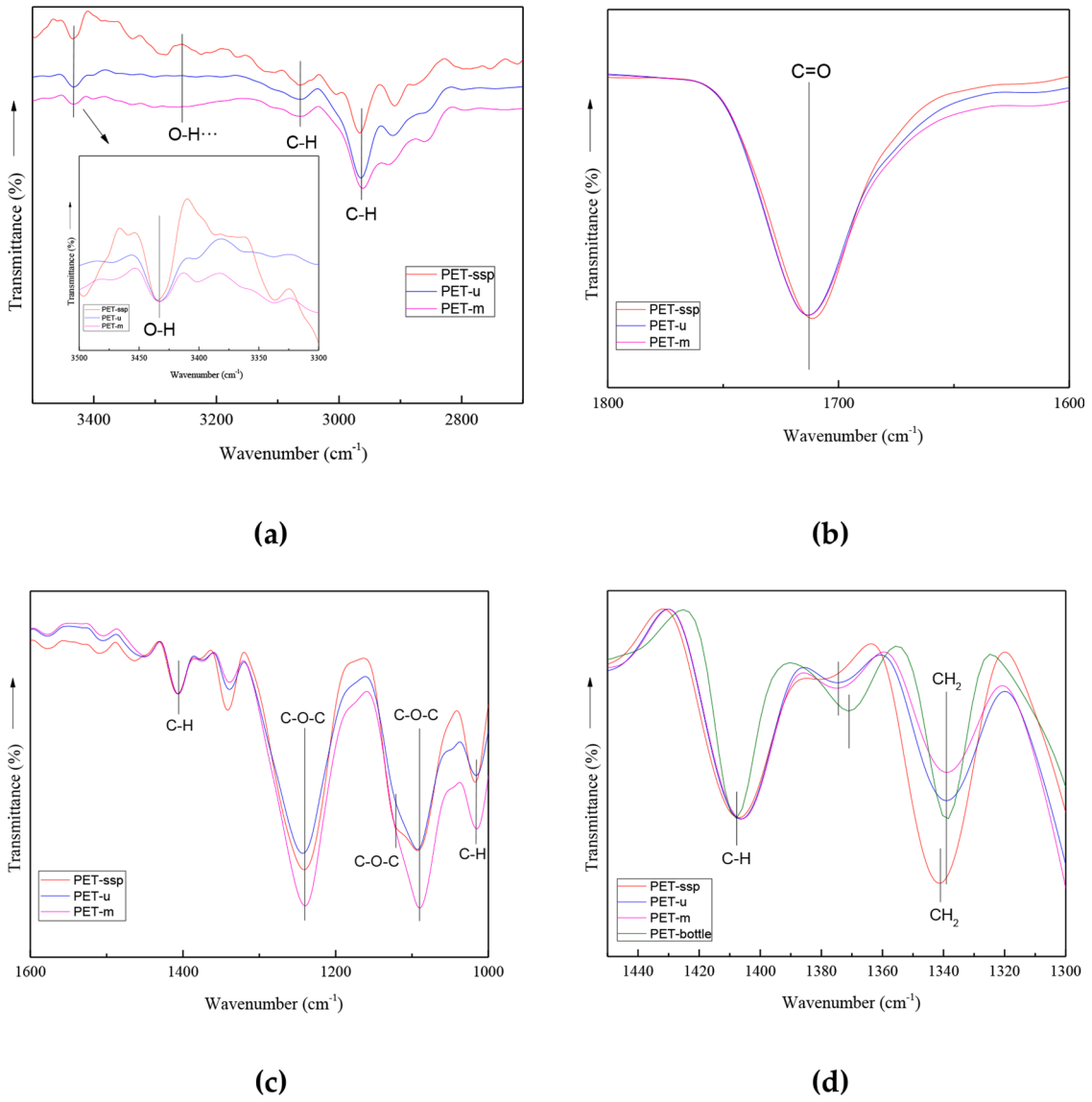

Fig. 4. FTIR spectra of PET-ssp, PET-u and PET-m at the intervals corresponding to: (a) the stretching vibration of hydroxyl group at 3500–2700 cm^{-1}, (b) carbonyl group at 1800–1600 cm^{-1}, (c) ester C-O-C group at 1600–1000 cm^{-1} and (d) spectra of PET-ssp, PET-u and PET-m samples and PET-bottle for comparison, at the interval corresponding to the CH_2 wagging region (1450–1300 cm^{-1}).

exothermic crystallization peak has been observed, thus confirming that the material is fully crystallized after post-condensation (Bartolotta et al., 2003). These results agree with those observed in FTIR analysis. Moreover, PET-ssp has shown a T_g value at 81°C, slightly higher than the observed in PET-v, due to the mobility restrictions imposed by the higher crystallinity. The two melting peaks observed in PET-ssp at 237 and 252°C, suggest different crystalline structures formed probably during post-condensation (Awaja and Pavel, 2005; Rajendran and Mishra, 2007; Tan et al., 2000). Even if PET-v can crystallize during heating, the melting enthalpy value is lower than that for PET-ssp, which confirmed its higher crystallinity.

PET-u and PET-m have shown a T_g at 82 and 77°C, respectively, in the range of that observed for PET-ssp, as well as the absence of exothermic crystallization. Regarding crystallinity of both PET-u and PET-m, they have shown lower melting enthalpy, and therefore lower crystallinity comparing with PET-ssp, agreeing with FTIR results. Moreover both have shown a single melting peak at higher temperature, suggesting a different polymer chain arrangement. In the same way than for FTIR analysis, a piece taken from a PET bottle has been analysed by DSC for comparative purposes. Data are summarized in Table 1. Results have confirmed that the differences in crystallinity among PET-u and PET-m and PET-ssp, in addition to the hydrolytic degradation, would also be influenced by processing.

In the cooling scan, all PET samples, with the exception of PET-ssp, have shown a pronounced sharp exothermic peak attributed to the crystallization process of PET. Comparing non degraded PET-v and PET-ssp, the higher crystallization temperature and exothermic enthalpy values observed in PET-v suggest a faster crystallization kinetic, which could be attributed to its lower molecular weight. Regarding cooling traces of PET-u and PET-m wastes, both crystallization temperature and crystallization enthalpy are higher than in the case of PET-ssp, also higher than PET-bottle, due to the higher mobility of chains that favoured the crystallization process. Moreover, only PET-ssp has shown a clear T_g around 76°C, related to the presence of amorphous fractions of PET due to its lower crystallization kinetics.

Finally, comparing the second heating scans with the first ones, the main differences have been found for PET-v and PET-ssp samples. The crystallization peak observed in the first scan for PET-v is hardly appreciated in the second one, suggesting that PET-v almost fully crystallizes during the cooling scan, while in the case of PET-ssp a clear

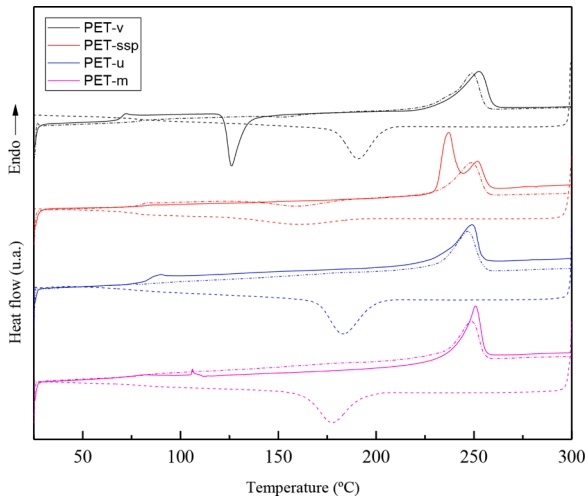

Fig. 5. DSC thermograms of different samples. First heating scan (–), cooling scan (—) and second heating scan (–•–•).

Table 1
Main parameters obtained from DSC thermograms of PET-v, PET-ssp, PET-u, PET-m, and PET-bottle during the 1st heating scan, cooling and 2nd heating scan.

		PET-v	PET-ssp	PET-u	PET-m	PET-bottle
1st heating scan	**T_g (°C)**	70	81	82 ± 3	77 ± 3	80
	T_c (°C)	126	-	-	-	99
	ΔH_c (J/g)	25	-	-	-	1
	T_m (°C)	253	237, 252	250 ± 2	250 ± 1	247
	ΔH_m (J/g)	36	46	37 ± 6	39 ± 4	37
	X_c (%)	8	34	27 ± 7	29 ± 4	27
Cooling scan	**T_g (°C)**	-	76	-	-	-
	T_c (°C)	191	161	188 ± 13	185 ± 12	178
	ΔH_c (J/g)	30	13	38 ± 3	38 ± 4	9
	X_c (%)	22	10	28 ± 3	28 ± 4	7
2nd heating scan	**T_g (°C)**	75	81	80 ± 1	80 ± 1	80
	T_c (°C)	153	160	-	-	-
	ΔH_c (J/g)	1	10	-	-	-
	T_m (°C)	249	248	248 ± 1	248 ± 0	243
	ΔH_m (J/g)	34	31	35 ± 4	34 ± 5	30
	X_c (%)	24	23	26 ± 4	25 ± 6	22

crystallization peak is observed at 160°C, absent in the first scan, thus corroborating its semi crystalline state. On the other hand, PET-ssp sample shows a single melting peak, due to, neither in the cooling scan nor during the second heating scan, the sample is not able to develop the same crystalline structure achieved in the post-condensation process. PET-bottle also shows slightly lower crystallinity in the second scan. However, comparing the melting enthalpies and crystallization degrees of PET-u and PET-m with those of PET-bottle, slightly higher values have been measured for PET-u and PET-m once the thermal history has been erased.

Degradation is also observed in plaques obtained by compression molding (Fig. 6).

As it can be seen, PET-u and PET-m presented different appearance when compared with PET-v and PET-ssp. Moreover, PET-m showed an intense brown color, which confirm a severe thermo-oxidative degradation during compression (Masmoudi et al., 2018b). Yellowing or discoloration of PET samples has been attributed in the literature to

Fig. 6. Images of PET samples obtained by compression molding. From left to right: PET-ssp, PET-v, PET-u and PET-m.

various degradations including thermo-oxidation (Berg et al., 2016), hydrolytic degradation (Gewert et al., 2015) and photo-oxidation (Duvall, 1995; Gewert et al., 2015). According to Gewert et al (2015), photo-degradation leads to the cleavage of the ester bond forming a carboxylic acid end group and a vinyl end group directly, or to radicals, which finally lead to the formation of a carboxylic acid end group. These carboxylic acid end groups have a promoting effect on thermo-oxidative degradation (Gewert et al., 2015), as occurred in PET-m sample. Then, the higher degradation of PET-m sample is confirmed, in good agreement with the FTIR analysis.

In order to analyse the effect of degradation, WCA analysis has also been performed. Obtained values, together with the images corresponding to the water drop over samples are shown in Table 2. A contact angle of 72° has been obtained for PET-v, while PET-ssp one presented a value of 77°. The post-condensation process, besides increasing the molecular weight, has decreased the amount of -COOH and -OH groups, thus decreasing the hydrophilicity, giving rise to a greater contact angle (Karayannidis et al., 1993). Regarding PET wastes, it can be observed that, the higher the degradation of PET, the lower the contact angle, especially for PET-m, showing higher hydrophilicity. This idea is in agreement with the conclusions about degradation obtained from FTIR analysis. In fact, hydrolytic and photo-oxidative degradation and thermo-oxidative as well for compression molded samples, resulted into the breaking of chains increasing the content of -COOH and -OH groups. As WCA results suggest, those functional groups could also be present at the surface and, consequently, interact with water decreasing the contact angle.

Regarding MFI values, it is well known that high values could be related with some degradation (de Oliveira Santos et al., 2014). Measured values are shown in Table 3. As PET-m sample has shown the highest value, it seems to be the most degraded sample, in agreement with previous results.

As the viscosity of PET products is a key parameter for their recycling, their intrinsic viscosity (I.V.) has also been determined according to Eq. (2) and gathered in Table 3. The experimentally obtained values for PET-v and PET-ssp are in the range of those provided by the supplier. The I.V. value decreased considerably for PET-m compared to starting PET-ssp, as can be seen in Table 3. Moreover, M_n and M_w values determined according to Eqs. (3) and 4, have confirmed that the residues of PET present a lower molecular weight, as was previously mentioned. PET-u and PET-m have shown higher MFI values and, therefore, they have present lower viscosity and molecular weight values, in agreement with the conclusions extracted from FTIR, DSC and WCA. As can be seen in Table 3, PET-ssp presents higher viscosity and molecular weight when compared to PET-v, due to the post-condensation process.

FTIR, DSC, WCA, and MFI results suggest that PET-u and PET-m samples have developed degradation that has caused chain cleavage, increasing crystallinity and hydrophilicity, and decreasing I.V. and the molecular weight. Therefore, the PET-u and PET-m samples analyzed do not have the properties required to be reused as raw material in common PET applications. This is why chemical recycling can be an alternative for degraded PET waste. However, the degradation experienced could affect the glycolysis process itself.

3.2. *Glycolysis process for BHET obtention*

Chemical recycling by depolymerization has been carried out in

Table 2
Contact angle values for different PET samples, together with the corresponding images of water drop over the samples.

PET-v	PET-ssp	PET-u	PET-m
Contact angle (°)			
72 ± 3	77 ± 3	71 ± 2	66 ± 3
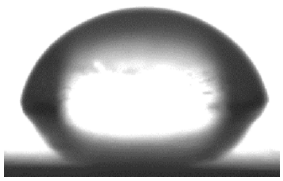	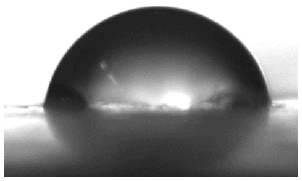	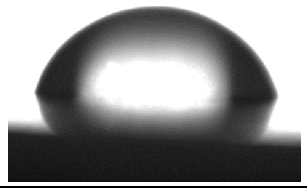	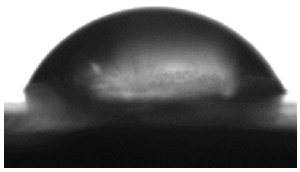

Table 3
Measured MFI values, together with the corresponding I.V. and M_n and M_w values for different PET samples.

Samples	MFI (g/10 min)	I.V. (dl/g)	M_n (g/mol)	M_w (g/mol)
PET-v	97 ± 32	0.60 ± 0.05	28228 ± 3998	37281 ± 6444
PET-ssp	39 ± 13	0.74 ± 0.08	33116 ± 6912	50833 ± 11377
PET-u	89 ± 14	0.60 ± 0.02	24780 ± 1600	37206 ± 2578
PET-m	126 ± 15	0.55 ± 0.02	21997 ± 1549	32740 ± 2475

Table 4
Insoluble fractions in THF and yield values of glycolysis products for each of the PET samples.

Fraction	Insoluble (%)	η (%)
G-v	3	68 ± 9
G-ssp	4	65 ± 11
G-u	3	55 ± 13
G-m	4	63 ± 10

order to find an alternative solution for degraded PET waste management and obtain BHET monomer for further polymer synthesis. Fig. 7a shows the aspect of glycolysis products just after the reaction and before the filtration process. It can be seen that the most degraded PET-u and PET-m samples presented a darker colour, attributed to the coloration observed in PET flakes. In the filtration process, most of the dark colour responsible fractions have been washed out with the water and removed together with the EG if it is compared with the darker glycolyzed product obtained from the PET-m glycolysis (Fig. 7b).

The glycolyzed products obtained after the filtration process have been analysed by FTIR. Obtained spectra can be seen in Fig. 7, together with those corresponding to PET-v and BHET. The spectrum of BHET monomer used as reference shows an absorption band around 3442 cm^{-1} related with the –OH group stretching vibration, which is also observed in the glycolyzed products, while it is not appreciated in the polymerized PET sample. Moreover, a double band related with the ester group carbonyl stretching vibration can be seen at 1712 cm^{-1} in the spectra of reference BHET sample and the glycolyzed products, whereas PET samples show single band. It seems that for all PET samples, after 30 min of glycolysis reaction, apart from oligomers, BHET monomer has been obtained, as will be corroborated by GPC analysis.

The yields obtained for the different reactions are summarized in Table 4, together with the insoluble fractions. While the highest yield of BHET has been obtained for PET-v, the lowest one has corresponded to PET-u. On the other hand, it must be taken into account that, even if the glycolyzed obtained from PET-m (G-m) presented a higher yield comparing with the glycolyzed obtained from PET-u (G-u), G-m presented the highest insoluble fraction. Fig. 8

Molecular weight values of the glycolysis products obtained have been measured by GPC. Fig. 9 shows the GPC traces obtained, together with that corresponding to BHET. Oligomer contents, obtained by integrating the area under the peak, are summarized in Fig. 9, where O1, O2 and O3 correspond to the fractions of BHET monomer, dimer and oligomer, respectively, with retention times of 38, 37 and 36 min (Fang et al., 2018; López-Fonseca et al., 2011).

Among the three different signals shown, that corresponding to O1 is the most significant one, corresponding to a M_w of 172-180 g/mol, related to BHET monomer (López-Fonseca et al., 2011). Peaks with lower intensity appeared around 36-38 min, related to BHET oligomers with 2-3 repeating units: the O2 fraction with a corresponding M_w of 384-396 g/mol, and the O3 one, with a corresponding M_w of 594-671 g/mol. As it can be seen from Fig. 9, BHET has been the main product

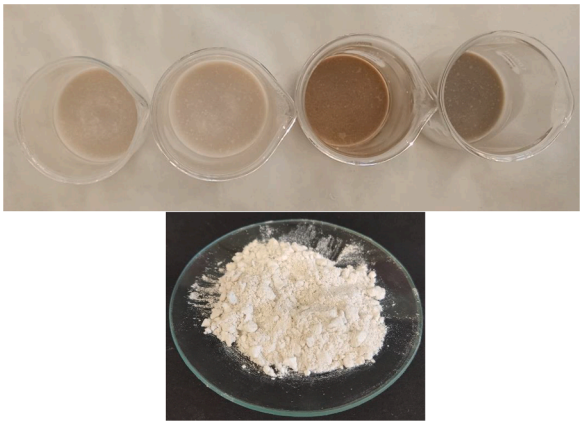

Fig. 7. (a) Image of the glycolysis products obtained from the depolymerization reactions of PET-v, PET-ssp, PET-u and PET-m (from the left to the right) and (b) glycolyzed G-m fraction after purification step.

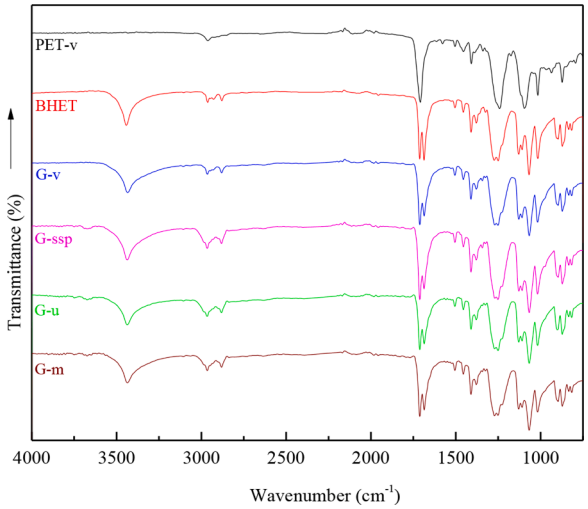

Fig. 8. FTIR spectra of the glycolyzed products obtained from the depolymerization reaction of different PET samples, together with those corresponding to PET-v and commercial BHET.

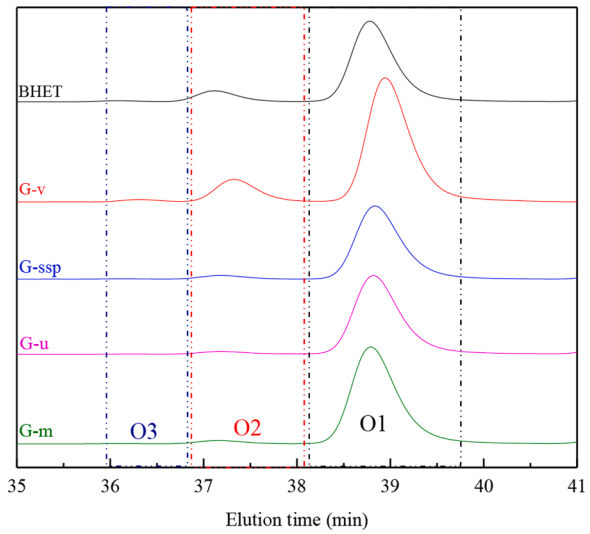

Fig. 9. GPC results comparing reference BHET and the BHET obtained from the depolymerization of different PET.

obtained from the glycolysis. Moreover, the most degraded PET-u and PET-m samples, presented a lower fraction of O2 dimers, which could be related to the fact that degradation consists on the breakdown of polymer chains into lower molar mass oligomers.

Table 5 summarizes the fractions of BHET monomer, dimer and oligomer obtained from the glycolysis of different PET samples at 30 min of reaction. By analysing the results, it can be concluded that PET-ssp and related residues present higher BHET content in the glycolyzed product obtained. Glycolyzed products of PET-ssp and their residues show similar composition, being 2 % higher the content of BHET for the most degraded PET-m and PET-u samples. On the other hand comparing G-u and G-m compositions with G-v, BHET content is even higher, reaching a value of 13 %. Therefore, for undegraded PET samples, the percentage of BHET monomer in G-ssp is almost 11% higher than in G-v, which could be related to the different structure of PET-v and PET-ssp. As observed in the DSC study, the PET-ssp sample presents two melting peaks at 237 and 252°C, the first being the most significant and occurring at a melting temperature lower than that observed in the rest of PET samples, which is attributed to the different crystal structures that have been generated in the post-condensation process (Tan et al., 2000). This lower melting temperature may favour the depolymerization of PET to BHET, being able to start the reaction earlier, obtaining a higher content of BHET after 30 min of reaction. However, it should be noted that the depolymerization reaction of PET to BHET monomer and dimer is reversible, and in the presence of EG, the amount of monomer and dimer changes in a matter of minutes, according to our previous work where the kinetics of the depolymerization reaction was studied between 10 and 180 min (Mendiburu-Valor et al., 2021). These results indicate that PET life cycle can be optimized by designing the glycolysis depolymerization reaction, not only controlling the parameters but also the raw materials, in order to obtain tailor made molecules for next resin production.

Table 5
Oligomer content (%) and M_w and M_n values, as obtained by GPC.

Samples	O1) M_n = 168-176 g/mol M_w = 172- 180 g/mol (%)	O2 M_n = 380-393 g/mol M_w = 384-396 g/mol (%)	O3) M_n = 591-649 g/mol M_w = 594-671 g/mol (%)
BHET ref	88	11	1
G-v	84	14	2
G-ssp	95	5	1
G-u	97	3	0
G-m	97	3	0

4. Conclusions

Different PET samples have been characterized in order to evaluate the effect of degradation on their physic-chemical properties. The photo-degradation and hydrolysis seems to be the main degradation process suffered by samples, causing the cleavage of polymer chains, leading to the formation of carboxylic and hydroxyl end groups, as has been corroborated by FTIR analysis. It has been confirmed by FTIR and DSC that the crystallinity is similar for the wastes and PET-bottle samples. In contrast, the post-condensed PET sample has a higher degree of crystallinity and a double melting peak in the DSC at a lower temperature due to the different crystal structures. Moreover, this fact causes the increasing of BHET content for PET-ssp samples respect to PET-v due to its lower melting temperature. It has also been shown that the degradation could also benefit the depolymerization of PET for the obtaining of BHET.

The results obtained in the WCA seem to confirm that PET-m and PET-u were degraded. Degradation in the environment generated -COOH and -OH groups as a consequence of photo-degradation and hydrolysis mechanisms. Furthermore, these functional groups promoted the thermo-degradation of the samples obtained by compression molding for WCA analysis. MFI values were also in accordance, the most degraded PET-m and PET-u samples presenting higher MFI values and therefore, lower viscosity and molecular weight, comparing with PET-ssp and PET-v. The results confirm that changes of PET in the marine environment as a consequence of UV radiation and seawater lead to greater degradation than in the case of municipal waste.

On the other hand, the glycolysis of PET waste has been carried out successfully, obtaining very good results, demonstrating that chemical recycling is a possible option for degraded materials, obtaining BHET for very short reaction times. In addition, it has been shown that the degradation of materials could change the properties of PET, leading in this case to an increase of BHET monomer content in glycolyzed products, reducing dimer and oligomer amounts. Obtained results suggest that BHET monomer content strongly depends on the selected raw materials.

Funding

This research received no external funding

Institutional review board statement

Not applicable.

Informed consent statement

Not applicable.

Data availability statement

The data presented in this study are available on request from the corresponding author.

CRediT authorship contribution statement

Eider Mendiburu-Valor: Methodology, Investigation, Writing – original draft, Visualization, Formal analysis. **Gurutz Mondragon:** Methodology, Investigation. **Nekane González:** Resources, Supervision. **Galder Kortaberria:** Methodology, Investigation, Writing – original draft. **Loli Martin:** Methodology, Investigation. **Arantxa Eceiza:** Conceptualization, Methodology, Supervision, Writing – review & editing, Visualization, Formal analysis, Funding acquisition. **Cristina Peña-Rodriguez:** Conceptualization, Methodology, Supervision,

Writing – original draft, Visualization, Formal analysis, Funding acquisition.

Declaration of Competing Interest

The authors declare that they have no known competing financial interests or personal relationships that could have appeared to influence the work reported in this paper.

Acknowledgments

Financial support from the University of the Basque Country in the frame of GIU18/216 and from the Provincial Council of Gipuzkoa (ItsasMikro project) are gratefully acknowledged. Authors thank the Circular Economy University-Company Classroom (Faculty of Engineering Gipuzkoa, UPV/EHU, Provincial Council of Gipuzkoa). Moreover, we are grateful to the Macrobehaviour-Mesostructure-Nanotechnology SGIker unit of UPV/EHU. Eider Mendiburu Valor thanks Basque Government for PhD grant (PRE_2018_1_0014).

References

Abbasi, M., Mojtahedi, M.R.M., Khosroshahi, A., 2007a. Effect of spinning speed on the structure and physical properties of filament yarns produced from used PET bottles. Journal of Applied Polymer Science 103. https://doi.org/10.1002/app.25369.

Abbasi, M., Mojtahedi, M.R.M., Khosroshahi, A., 2007b. Effect of spinning speed on the structure and physical properties of filament yarns produced from used PET bottles. Journal of Applied Polymer Science 103. https://doi.org/10.1002/app.25369.

Ahani, M., Khatibzadeh, M., Mohseni, M., 2016. Preparation and characterization of poly (ethylene terephthalate)/hyperbranched polymer nanocomposites by melt blending. Nanocomposites 2. https://doi.org/10.1080/20550324.2016.1187966.

Awaja, F., Pavel, D., 2005. Recycling of PET. Eur. Polym. J. 41, 1453–1477. https://doi.org/10.1016/J.EURPOLYMJ.2005.02.005.

Barnes, D.K.A., Galgani, F., Thompson, R.C., Barlaz, M., 2009. Accumulation and fragmentation of plastic debris in global environments. Philos. Trans. R. Soc. B Biol. Sci. 364 https://doi.org/10.1098/rstb.2008.0205.

Bartolotta, A., di Marco, G., Farsaci, F., Lanza, M., Pieruccini, M., 2003. DSC and DMTA study of annealed cold-drawn PET: a three phase model interpretation. Polymer (Guildf) 44, 5771–5777. https://doi.org/10.1016/S0032-3861(03)00589-5.

Berg, D., Schaefer, K., Koerner, A., Kaufmann, R., Tillmann, W., Moeller, M., 2016. Reasons for the discoloration of postconsumer poly(ethylene terephthalate) during reprocessing. Macromol. Mater. Eng. 301, 1454–1467. https://doi.org/10.1002/mame.201600313.

Bertoldo, M., Labardi, M., Rotella, C., Capaccioli, S., 2010. Enhanced crystallization kinetics in poly(ethylene terephthalate) thin films evidenced by infrared spectroscopy. Polymer (Guildf) 51, 3660–3668. https://doi.org/10.1016/J.POLYMER.2010.05.040.

Chapa-Martínez, C.A., Hinojosa-Reyes, L., Hernández-Ramírez, A., Ruiz-Ruiz, E., Maya-Treviño, L., Guzmán-Mar, J.L., 2016. An evaluation of the migration of antimony from polyethylene terephthalate (PET) plastic used for bottled drinking water. Sci. Total Environ. 565, 511–518. https://doi.org/10.1016/J.SCITOTENV.2016.04.184.

Chemie, 2020. Polyethylene Terephthalate (PET) Global Market to 2020 - Increasing Demand from Carbonated Soft Drinks. Food and Beer Packaging in BRIC Nations Driving Growth [WWW Document]. URL http://www.chemie.de/marktstudien/10877/polyethylene-terephthalate-pet-global-market-to-2020-increasing-demand-from-carbonated-soft-drinks-food-and-beer-packaging-in-bric-nations-driving-growth.html (accessed 12.20.19).

Cole, K.C., Ajji, A., Pellerin, É., 2002. New Insights into the Development of Ordered Structure in Poly(ethylene terephthalate). 1. Results from External Reflection Infrared Spectroscopy. Macromolecules 35. https://doi.org/10.1021/ma011492i.

de Oliveira Santos, R.P., Castro, D.O., Ruvolo-Filho, A.C., Frollini, E., 2014. Processing and thermal properties of composites based on recycled PET, sisal fibers, and renewable plasticizers. J. Appl. Polym. Sci. 131 https://doi.org/10.1002/app.40386.

del Mar Castro López, M., Ares Pernas, A.I., Abad López, M.J., Latorre, A.L., López Vilariño, J.M., González Rodríguez, M.V., 2014. Assessing changes on poly(ethylene terephthalate) properties after recycling: Mechanical recycling in laboratory versus postconsumer recycled material. Mater. Chem. Phys. 147, 884–894. https://doi.org/10.1016/J.MATCHEMPHYS.2014.06.034.

Dieval, F., Khoffi, F., Mir, R., Chaouch, W., le Nouen, D., Chakfe, N., Durand, B., 2012. Long-term biostability of pet vascular prostheses. Int. J. Polym. Sci. 2012 https://doi.org/10.1155/2012/646578.

Dubelley, F., Planes, E., Bas, C., Pons, E., Yrieix, B., Flandin, L., 2017. The hygrothermal degradation of PET in laminated multilayer. Eur. Polym. J. 87, 1–13. https://doi.org/10.1016/J.EURPOLYMJ.2016.12.004.

Duvall, D.E., 1995. Environmental degradation of pet and its potential effect on long-term mechanical properties of oriented pet products. Polym. Plast. Technol. Eng. 34, 227–242. https://doi.org/10.1080/03602559508015825.

Edge, M., Wiles, R., Allen, N.S., McDonald, W.A., Mortlock, S.V., 1996. Characterisation of the species responsible for yellowing in melt degraded aromatic polyesters—I: Yellowing of poly(ethylene terephthalate). Polym. Degrad. Stab. 53, 141–151. https://doi.org/10.1016/0141-3910(96)00081-X.

Fang, P., Liu, B., Xu, J., Zhou, Q., Zhang, S., Ma, J., lu, X., 2018. High-efficiency glycolysis of poly(ethylene terephthalate) by sandwich-structure polyoxometalate catalyst with two active sites. Polym. Degrad. Stab. 156, 22–31. https://doi.org/10.1016/J.POLYMDEGRADSTAB.2018.07.004.

Fotopoulou, K.N., Karapanagioti, H.K., 2019. Degradation of various plastics in the environment. Handbook of Environmental Chemistry. Springer Verlag, pp. 71–92. https://doi.org/10.1007/698_2017_11.

Gantillon, B., Spitz, R., McKenna, T.F., 2004. The solid state postcondensation of PET, 1. Macromol. Mater. Eng. 289 https://doi.org/10.1002/mame.200300289.

Gewert, B., Plassmann, M.M., Macleod, M., 2015. Pathways for degradation of plastic polymers floating in the marine environment. Environ. Sci. Process. Impacts. https://doi.org/10.1039/c5em00207a.

Holland, B.J., Hay, J.N., 2002. The thermal degradation of PET and analogous polyesters measured by thermal analysis–Fourier transform infrared spectroscopy. Polymer (Guildf) 43, 1835–1847. https://doi.org/10.1016/S0032-3861(01)00775-3.

Iñiguez, M.E., Conesa, J.A., Fullana, A., 2018a. Recyclability of four types of plastics exposed to UV irradiation in a marine environment. Waste Management 79, 339–345. https://doi.org/10.1016/J.WASMAN.2018.08.006.

Iñiguez, M.E., Conesa, J.A., Soler, A., 2018b. Effect of marine ambient in the production of pollutants from the pyrolysis and combustion of a mixture of plastic materials. Marine Pollution Bulletin 130, 249–257. https://doi.org/10.1016/J.MARPOLBUL.2018.03.040.

Karayannidis, G.P., Kokkalas, D.E., Bikiaris, D.N., 1993. Solid-state polycondensation of poly(ethylene terephthalate) recycled from postconsumer soft-drink bottles I. J. Appl. Polym. Sci. 50 https://doi.org/10.1002/app.1993.070501213.

López-Fonseca, R., Duque-Ingunza, I., de Rivas, B., Flores-Giraldo, L., Gutiérrez-Ortiz, J. I., 2011. Kinetics of catalytic glycolysis of PET wastes with sodium carbonate. Chem. Eng. J. 168, 312–320. https://doi.org/10.1016/J.CEJ.2011.01.031.

Masmoudi, F., Fenouillot, F., Mehri, A., Jaziri, M., Ammar, E., 2018a. Characterization and quality assessment of recycled post-consumption poly(ethylene terephthalate) (PET). Environmental Science and Pollution Research 25. https://doi.org/10.1007/s11356-018-2390-7.

Masmoudi, F., Fenouillot, F., Mehri, A., Jaziri, M., Ammar, E., 2018b. Characterization and quality assessment of recycled post-consumption poly(ethylene terephthalate) (PET). Environmental Science and Pollution Research 25. https://doi.org/10.1007/s11356-018-2390-7.

Mendiburu-Valor, E., Mondragon, G., González, N., Kortaberria, G., Eceiza, A., Peña-Rodriguez, C., 2021. Improving the efficiency for the production of bis-(2-hydroxyethyl) terephtalate (BHET) from the glycolysis reaction of poly(ethylene terephtalate) (PET) in a Pressure Reactor. Polymers (Basel) 13. https://doi.org/10.3390/polym13091461.

Pegoretti, A., Penati, A., 2004. Effects of hygrothermal aging on the molar mass and thermal properties of recycled poly(ethylene terephthalate) and its short glass fibre composites. Polym. Degrad. Stab. 86, 233–243. https://doi.org/10.1016/J.POLYMDEGRADSTAB.2004.05.002.

Peña-Rodriguez, C., Mondragon, G., Mendoza, A., Mendiburu-Valor, E., Eceiza, A., Kortaberria, G., 2021. Recycling of marine plastic debris. Recent Developments in Plastic Recycling. Springer. https://doi.org/10.1007/978-981-16-3627-1_6.

Pirzadeh, E., Zadhoush, A., Haghighat, M., 2007. Hydrolytic and thermal degradation of PET fibers and PET granule: the effects of crystallization, temperature, and humidity. J. Appl. Polym. Sci. 106 https://doi.org/10.1002/app.26788.

Plastics Recyclers Europe, 2020. Marine Litter [WWW Document]. URL https://www.plasticsrecyclers.eu/marine-litter (accessed 5.9.20).

Plastics Recyclers Europe, Natural Mineral Waters Europe, PETCORE Europe, UNESDA Soft Drinks Europe, 2022. PET Market in Europe state of play 2022, collection and recycling [WWW Document]. URL https://www.plasticsrecyclers.eu/plastics-recyclers-publications (accessed 4.20.22).

PlasticsEurope, 2020. Plastics—the Facts 2020 [WWW Document]. URL https://plasticseurope.org/knowledge-hub/plastics-the-facts-2020/(accessed 12.15.19).

Qin, Y., Qu, M., Kaschta, J., Schubert, D.W., 2018. Comparing recycled and virgin poly (ethylene terephthalate) melt-spun fibres. Polym. Test. 72 https://doi.org/10.1016/j.polymertesting.2018.10.028.

Raheem, A.B., Noor, Z.Z., Hassan, A., Abd Hamid, M.K., Samsudin, S.A., Sabeen, A.H., 2019. Current developments in chemical recycling of post-consumer polyethylene terephthalate wastes for new materials production: a review. J. Clean. Prod. 225, 1052–1064. https://doi.org/10.1016/J.JCLEPRO.2019.04.019.

Rajendran, S., Mishra, S.P., 2007. Chemical, structural and thermal changes in PET caused by solvent induced polymer crystallisation. Polym. Polym. Compos. 15 https://doi.org/10.1177/096739110701500203.

Sammon, C., Yarwood, J., Everall, N., 2000. An FT–IR study of the effect of hydrolytic degradation on the structure of thin PET films. Polym. Degrad. Stab. 67, 149–158. https://doi.org/10.1016/S0141-3910(99)00104-4.

Sanches, N.B., Dias, M.L., Pacheco, E.B.A.V., 2005. Comparative techniques for molecular weight evaluation of poly (ethylene terephthalate) (PET). Polym. Test. 24, 688–693. https://doi.org/10.1016/J.POLYMERTESTING.2005.05.006.

Shojaei, B., Abtahi, M., Najafi, M., 2020. Chemical recycling of PET: a stepping-stone toward sustainability. Polym. Adv. Technol. 31 https://doi.org/10.1002/pat.5023.

Starkweather, H.W., Zoller, P., Jones, G.A., 1983. The heat of fusion of poly(ethylene terephthalate). J. Polym. Sci. Polym. Phys. Ed. 21 https://doi.org/10.1002/pol.1983.180210211.

Tan, S., Su, A., Li, W., Zhou, E., 2000. New insight into melting and crystallization behavior in semicrystalline poly(ethylene terephthalate). J. Polym. Sci. Part B Polym. Phys. 38, 10.1002/(SICI)1099-0488(20000101)38:1<53::AID-POLB6>3.0.CO;2-G.

Venkatachalam, S., G., S., V., J., R., P., Rao, K., K., A., 2012. Degradation and Recyclability of Poly (Ethylene Terephthalate), in: Polyester. InTech. 10.5772/48612.

Wei, H.sen, Liu, K.T., Chang, Y.C., Chan, C.H., Lee, C.C., Kuo, C.C., 2017. Superior mechanical properties of hybrid organic-inorganic superhydrophilic thin film on plastic substrate. Surf. Coat. Technol. 320, 377–382. https://doi.org/10.1016/J.SURFCOAT.2016.12.025.

Zhou, X., Wang, C., Fang, C., Yu, R., Li, Y., Lei, W., 2019. Structure and thermal properties of various alcoholysis products from waste poly(ethylene terephthalate). Waste Manag. 85, 164–174. https://doi.org/10.1016/J.WASMAN.2018.12.032.